Journal of Molecular Structure 1099 (2015) 297–303

Contents lists available at ScienceDirect

Journal of Molecular Structure

journal homepage: http://www.elsevier.com/locate/molstruc

Rhodium(III)-triphenylphosphine complex with NNS donor thioether containing Schiff base ligand: Synthesis, spectra, electrochemistry and catalytic activity

Sujan Biswas, Deblina Sarkar, Subhankar Kundu, Puspendu Roy, Tapan Kumar Mondal*

Inorganic Chemistry Section, Department of Chemistry, Jadavpur University, Kolkata 700032, India

ARTICLE INFO

Article history:
Received 14 February 2015
Received in revised form
25 May 2015
Accepted 22 June 2015
Available online 29 June 2015

Keywords:
Rhodium(III)-triphenylphosphine complex
Thioether containing NNS donor ligand
X-ray structure
Electrochemistry
Transfer hydrogenation of ketones
DFT calculation

ABSTRACT

New rhodium(III)-triphenylphosphine complex, $[Rh(PPh_3)(L)Cl_2](PF_6)$ (**1**) with thioether containing NNS donor ligand (L) (L = 2-(methylthio)-N-((pyridine-2-yl)methylene)benzenamine) has been synthesized and characterized. The pseudo octahedral geometry of the complex has been confirmed by single crystal X-ray analysis. The electronic structure, redox properties, absorption and emission properties of the complexes have been interpreted by DFT and TDDFT calculations. The complex effectively catalyzed the transfer hydrogenation reaction of ketones in 2-propanol and oxidation of alcohols in presence of NMO.

1. Introduction

The transition metal complexes with π-acidic diimine (-N=C–C=N-) functional polypyridyl ligands display exciting photochemical and photophysical properties, and have applications in many technological fields [1–7]. The excited states of these compounds are often sufficiently long-lived to become engaged in energy transfer reactions. Their electroluminescent properties have been applied in solar energy converters [8] and as electroluminescent materials in OLED-type devices [4,9–14]. The compounds have been used as luminescent probes for long-range electron-transfer studies in proteins and other biomolecular systems [15–18], and light-emitting electronic devices [19–21]. In recent years, several groups have used polydentate ligands with thioether moieties for the synthesis of model complexes to mimicking the spectroscopic and structural properties of the active sites of metallo proteins [22–25]. Chelating ligands containing N,N,S donor atoms have unique interest in the coordination chemistry because of the stability, chemical and electrochemical activities and diversity in binding to metal ions [26–37].

Transition metal complexes are powerful catalysts for various organic transformations. A number of transition metal complexes are known to catalyze transfer hydrogenation of ketones [38–42]. Over the last few decades significant effort on hydrogenation has been given on the use of ruthenium, rhodium and iridium catalysts [40–43]. The transition metal complexes play important roles in the oxidative processes employed in chemical industry and laboratory synthesis [44]. With this view there has been a growing interest in transition metal catalyzed oxidation of alcohols using oxidants such as molecular oxygen, iodosylbenzene, hydrogen peroxide, *tert*–butyl hydroperoxide and N–methylmorpholine–N–oxide (NMO) [45–50].

Transition metal complexes have been widely used as potential catalysts for various organic transformation reactions those are otherwise difficult to achieve or even impossible. In recent past, we have witnessed significant progress in development of new ruthenium, rhodium and iridium metal-catalyzed reactions [38–43]. Rhodium and iridium complexes have been proven to lead very efficient processes having potential industrial applications [43]. Herein, we report the synthesis and spectral characterization of new octahedral rhodium(III) triphenylphosphine complex $[Rh(PPh_3)(L)Cl_2](PF_6)$ (**1**) (where L = 2-(methylthio)-N-((pyridine-2-yl)methylene)benzenamine). The structure has been confirmed by single crystal X-ray study of **1**. The electronic transitions,

* Corresponding author.
E-mail address: tkmondal@chemistry.jdvu.ac.in (T.K. Mondal).

http://dx.doi.org/10.1016/j.molstruc.2015.06.065
0022-2860/

assignment of spectral bands and redox properties have been interpreted by DFT and TDDFT calculations. We also report the catalytic transfer hydrogenation of ketones with 2-propanol and oxidation of alcohols with N–methylmorpholine–N–oxide (NMO).

2. Experimental

2.1. Materials

2-(methylthio)-N-((pyridine-2-yl)methylene)benzenamine (L) was prepared following the published procedure [35]. Pyridine-2-carboxaldehyde and 2-aminothiophenol were purchased from Sigma Aldrich, and used as received. All other chemicals and solvents were of reagent grade and were used without further purification.

2.2. Physical measurements

Microanalyses (C, H, N) were performed using a Perkin–Elmer CHN-2400 elemental analyzer. The electronic spectra were measured on Lambda 750 Perkin Elmer spectrophotometer in acetonitrile solution. The IR spectra were recorded on RX-1 Perkin Elmer spectrophotometer in the spectral range 4000–400 cm^{-1} with the samples in the form of KBr pellets. Luminescence property was measured using LS-55 Perkin Elmer fluorescence spectrophotometer at room temperature (298 K) in acetonitrile solution by 1 cm path length quartz cell. Fluorescence lifetimes were measured using a time-resolved spectrofluorometer from IBH, UK. The instrument uses a picoseconds diode laser (NanoLed-03, 370 nm) as the excitation source and works on the principle of time-correlated single photon counting [51]. The goodness of fit was evaluated by χ^2 criterion and visual inspection of the residuals of the fitted function to the data. ^{1}H NMR spectra were recorded in $CDCl_3$ on Bruker 300 MHz FT-NMR spectrometers in presence of TMS as internal standard. Cyclic voltammetric measurements were carried out using a CH1 Electrochemical workstation. A platinum wire working electrode, a platinum wire auxiliary electrode and Ag/AgCl reference electrode were used in a standard three-electrode configuration. [nBu_4N][ClO_4] was used as the supporting electrolyte and the scan rate used was 50 mV s^{-1} in acetonitrile under dinitrogen atmosphere. Powder X-ray diffractions were performed on a Bruker D8 instrument with Cu Kα radiation.

The luminescence quantum yield was determined using carbazole as reference with a known ϕ_R of 0.42 in MeCN. The complex and the reference dye were excited at the same wavelength, maintaining nearly equal absorbance (~0.1), and the emission spectra were recorded. The area of the emission spectrum was integrated using the software available in the instrument and the quantum yield is calculated according to the following equation:

$$\phi_S/\phi_R = [A_S/A_R] \times [(Abs)_R/(Abs)_S] \times \left[\eta_S^2/\eta_R^2\right]$$

here, ϕ_S and ϕ_R are the luminescence quantum yield of the sample and reference, respectively. A_S and A_R are the area under the emission spectra of the sample and the reference respectively, $(Abs)_S$ and $(Abs)_R$ are the respective optical densities of the sample and the reference solution at the wavelength of excitation, and η_S and η_R are the values of refractive index for the respective solvent used for the sample and reference.

The catalytic conversion yields were determined by GC instrument equipped with a flame ionization detector (FID) using a HP–5 column of 30 m length, 0.53 mm diameter and 5.00 μm film thickness. The column, injector and detector temperatures were 200, 250 and 250 °C respectively. The carrier gas was N_2 (UHP grade) at a flow rate of 30 mL/min. The injection volume of sample was 2 μL. The oxidation products were identified by GC co-injection with authentic samples.

2.3. Preparation of [$Rh(PPh_3)(L)Cl_2$](PF_6) (1)

$RhCl_3.3H_2O$ (0.10 g, 0.379 mmol) was added to an acetonitrile solution of 2-(methylthio)-N-((pyridine-2-yl)methylene)benzenamine (L) (0.091 g, 0.395 mmol) and PPh_3 (0.104 g, 0.385 mmol). The reaction mixure was refluxed for 10 h under stirring condition. The solvent was removed under reduced pressure using a rotary evaporator. The red gummy mass was dissolved in minimum volume of methanol and aqueous solution of NH_4PF_6 was added to precipitate the product. The precipitate was filtered and washed with cold water, finally dried in vacuuo over P_4O_{10}. Yield was 0.197 g, 64%.

Anal. Calc. for $C_{31}H_{27}Cl_2F_6N_2P_2RhS$ (**1**): C, 46.00; H, 3.36; N, 3.46%. Found: C, 45.87; H, 3.31; N, 3.40%. IR data (KBr, cm^{-1}): 1594 υ(C=N), 842 $\upsilon(PF_6^-)$. ^{1}H NMR data ($CDCl_3$, ppm): 8.86 (1H, d, J = 4.2 Hz), 8.67 (1H, s), 8.41 (2H, d, J = 8.0 Hz), 7.87 (1H, t, J = 8.1 Hz), 7.12–7.52 (20H, m), 2.89 (3H, s). E (Rh^{III}/Rh^{IV}): 1.07 V; E_{pc}: −1.05 V.

2.4. Procedure for catalytic transfer hydrogenation

The ketone (1 mmol), KOH (2 mL of a 0.2 M solution in 2-propanol), and the complex (0.01 mmol dissolved in CH_3CN) were added to 10 mL of 2-propanol, and the mixture was refluxed for 4 h. 2-Propanol was removed on a rotary evaporator, and the resulting semisolid was extracted with diethyl ether (5 × 10 mL). The extract was passed through a short column of silica gel. The column was washed with ~100 mL of diethyl ether. All the eluates from the column were mixed, and the solvent from the mixture was evaporated off on a rotary evaporator. The resulting residue was dissolved in 2–3 mL of hexane and subjected to GC.

2.5. Procedure for catalytic oxidation of alcohols with NMO

A solution of complex (0.01 mmol) in CH_2Cl_2 (25 mL) was added to the mixture containing alcohol substrate (1 mmol), K_2CO_3 (1.3 mmol), solid NMO (3 mmol) and molecular sieves. The reaction mixture was refluxed for 3 h, and the solvent was then evaporated under reduced pressure. The residue was then extracted with diethyl ether (20 mL), concentrated to ≈ 1 mL. The oxidized product present in diethyl ether extract was analyzed by GC.

2.6. Computational details

Full geometry optimization was carried out using the density functional theory method at the B3LYP level for the representative complex **1a** [52,53]. All elements except rhodium were assigned the 6-31G(d) basis set. The LANL2DZ basis set with effective core potential was employed for the rhodium atom [54–56]. The vibrational frequency calculation was performed to ensure that the optimized geometry represents the local minima and there are only positive eigenvalues. All calculations were performed with Gaussian09 program package [57] with the aid of the GaussView visualization program. Vertical electronic excitations based on B3LYP optimized geometry were computed using the time-dependent density functional theory (TDDFT) formalism [58–60] in acetonitrile using conductor-like polarizable continuum model (CPCM) [61–63]. GaussSum [64] was used to calculate the fractional contributions of various groups to each molecular orbital.

2.7. Crystal structure determination and refinement

Details of crystal analysis, data collection and structure refinement data for [Rh(PPh_3)(L)Cl_2](PF_6) (**1**) is given in Table 1. Crystal mounting was done on glass fibers with epoxy cement. Single crystal data collections were performed with an automated Bruker SMART APEX CCD diffractometer using graphite monochromatized Mo Kα radiation (λ = 0.71073 Å). Reflection data were recorded using the ω scan technique. Unit cell parameters were determined from least-squares refinement of setting angles with θ in the range 2.08 ≤θ ≤ 26.73°. Out of 24532 collected data 2945 with I > 2σ (I) were used for structure solution within *hkl* parameters −13 ≤ *h* ≤ 11, −13 ≤ *k* ≤ 12, −20 ≤ *l* ≤ 21. The structures were solved and refined by full-matrix least-squares techniques on F^2 using the SHELXS-97 program [65]. The absorption corrections were done by the multi-scan technique. All data were corrected for Lorentz and polarization effects, and the non-hydrogen atoms were refined anisotropically. Hydrogen atoms were generated using SHELXL-97 [65] and their positions calculated based on the riding mode with thermal parameters equal to 1.2 and 1.5 times that of the associated aromatic and aliphatic C atoms, and participated in the calculation of the final R-indices.

3. Results and discussion

3.1. Synthesis and formulation

The pseudo octahedral [Rh(PPh_3)(L)Cl_2](PF_6) (**1**) complex (where L = 2-(methylthio)-N-((pyridine-2-yl)methylene)benzenamine) has been synthesized. The synthetic route of the complex is shown in Scheme 1. The reaction of $RhCl_3$ with L and PPh_3 in acetonitrile under refluxing condition results in the formation of red gummy mass of the complex. The solid product of the complex has been isolated by addition of aqueous NH_4PF_6 to the methanolic solution of the complex. The X-ray structure of the complex revels that the ligand binds through pyridyl-N, imine-N and thioether-S atoms to rhodium. Characterization of the complex is carried out by IR, NMR, UV–Vis and elemental analysis (*see experimental section*). The υ(C=N) stretching in the complex is significantly shifted to lower frequency region compare to free ligand value and observed at around 1594 cm^{-1} [35], supporting the coordination of imine-N to rhodium. A sharp peak at 842 cm^{-1} corresponds to the presence of PF_6^- (Fig. S1).

The ^{1}H NMR spectra of the complexes in $CDCl_3$ show multiple signals in the "aromatic" region due to the presence of PPh_3 group. The overlapping of many proton resonances due to their similar chemical shifts has prevented identification of individual proton signals of the aromatic protons; though the spectra show the calculated number of equivalent aromatic protons. But a sharp singlet at 2.89 ppm corresponding to S–Me group has been observed at downfield region compare to free ligand value supporting the coordination of thioether-S to rhodium [66].

3.2. Molecular structure

Single crystal suitable for structure determination was obtained by slow diffusion of n-hexane into dichloromethane solution of [Rh(PPh_3)(L)Cl_2](PF_6) (**1**). The crystallographic data collection and refinement parameters are given in Table 1; selected bond lengths and angles are given in Table 2. ORTEP plot with atomic numbering scheme is shown in Fig. 1. The rhodium atom adopts a distorted octahedral geometry; the ligand **L** is coordinated through pyridyl-N, imine-N and thioether-S atoms and other three sites are occupied by two *cis*-Cl and PPh_3 respectively. The deviation of the rhodium coordination sphere from the ideal octahedron is because of the small bite angle of almost co-planar (1.0 (4)°) five membered chelate rings, Rh1–N1–C5–C6–N2, 77.1 (4)° and Rh1–N2–C7–C12–S1, 84.0 (3)°. The Rh–N (pyridyl) bond, Rh (1)-N (1), 2.028 (11) Å is longer than the Rh–N (imine), Rh (1)-N (2), 1.972 (11) Å unlike the reverse Re–N bond distances reported previously [35]. The Rh1–S1 bond distance, 2.301 (12) Å is comparable to the reported Rh–S bond distances [67–69]. The crystal structure of **1** forms 1D-supramolecular chain by inter-molecular π … π interaction between the pyridyl (N1–C1–C2–C3–C4–C5) rings and pπ(Cl) … π interaction between the Cl and the phenyl (C7–C8–C9–C10–C11–C12) ring of coordinated ligand L with the distances of 3.390 (6) Å and 3.595 (6) Å respectively (Fig. 2).

Table 1
Crystallographic data and refinement parameters for [Rh(PPh_3)(L)Cl_2](PF_6) (**1**).

Empirical formula	$C_{31}H_{27}Cl_2N_2PRhS$, PF_6
Formula weight	809.37
Crystal system	Triclinic
Space group	*P-1*
a/Å	10.1608 (6)
b/Å	10.3719 (6)
c/Å	17.4630 (5)
α (°)	73.751 (4)
β (°)	77.008 (4)
γ (°)	75.913 (4)
V/Å^3	1689.28 (16)
Z	2
ρ_{calcd}/g cm^{-3}	1.591
μ/mm^{-1}	0.878
T/K	293 (2)
hkl range	−13–11, −13–12, −20–21
F (000)	812
θ range (°>)	2.08–26.73
Reflns collected	24532
Unique reflns (R_{int})	7092 (0.1192)
Observed data ($I > 2\sigma(I)$)	2945
Data/restraints/parameters	7092/0/406
R1[a], wR2[b] ($I > 2\sigma(I)$)	0.0861, 0.1683
R1, wR2 (all data)	0.0945, 0.2083
GOF[c]	1.169
Largest diff. peak/hole/e Å^{-3}	1.206/−1.004

[a] $R_1 = \sum(|F_o| - |F_c|)/\sum|F_o|$.
[b] $wR_2 = \{\sum[w(F_o^2 - F_c^2)^2]/\sum[w(F_o^2)^2]\}^{1/2}$, $w = 1/[\sigma^2(F_o^2) + (0.0295\,P)^2]$, where $P = (F_o^2 + 2\,F_c^2)/3$.
[c] GOF $= \{\sum[w(F_o^2 - F_c^2)^2]/(n - p)\}^{1/2}$, where n = number of measured data and p = number of parameters.

3.3. DFT calculation and electronic structure

The geometry of [Rh(PPh_3)(L)Cl_2]$^+$ (**1**$^+$) has been optimized in singlet state by the DFT method with the B3LYP hybrid functional. The optimized bond distances and angles are given in Table 2. The calculated bond parameters are well correlated with the X-ray crystal structure data.

The energy and compositions of selected molecular orbitals are given in Table 3. Contour plots of selected molecular orbitals are presented in Fig. 3. The higher energy molecular orbitals (HOMO, HOMO-1, HOMO-2 and HOMO-5) are composed by mixed dπ(Rh) (16–24%) and pπ(Cl) (46–62%) orbitals. The HOMO-8 and HOMO-10 have mixed π(L) and π(PPh_3) character. The LUMO has 95% π*(L) character with major contribution of imine (C=N) function. The LUMO + 1 and LUMO + 2 have 41–48% dπ(Rh) character along with reduced contributions from π*(L) and pπ(Cl) orbitals.

3.4. TDDFT calculation and electronic spectra

The solution spectrum of the complex, [Rh(PPh_3)(L)Cl_2](PF_6) (**1**) in acetonitrile shows one moderately intense broad band at 418 nm along with two peaks at 330 and 270 nm (Fig. 4). To assign the

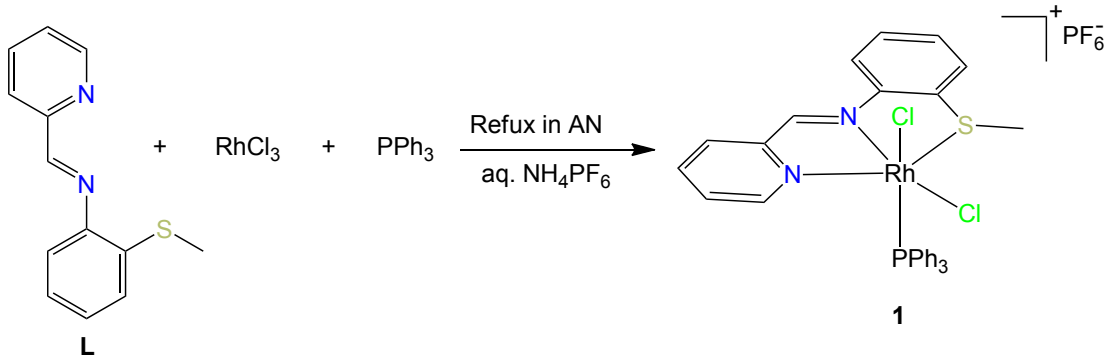

Scheme 1. Synthesis of $[Rh(PPh_3)(L)Cl_2](PF_6)$ (**1**) complex.

Table 2
Selected X–ray and calculated bond distance (Å) and angles (°) of **1**.

Bonds (Å)	X–ray	Calc.
Rh1–Cl1	2.284 (8)	2.336
Rh1–Cl2	2.325 (7)	2.358
Rh1–S1	2.301 (12)	2.340
Rh1–N1	2.028 (11)	2.058
Rh1–N2	1.972 (11)	2.027
Rh1–P1	2.387 (5)	2.433
C6–N2	1.271 (11)	1.295
Angles (°)		
N1–Rh1–Cl1	97.7 (4)	96.03
N1–Rh1–Cl2	84.6 (3)	85.57
N1–Rh1–P1	99.0 (3)	95.66
N1–Rh1–S1	160.9 (4)	163.3
N1–Rh1–N2	77.1 (4)	78.55
N2–Rh1–Cl1	172.3 (4)	173.9
N2–Rh1–Cl2	85.1 (3)	85.17
N2–Rh1–P1	99.8 (4)	96.84
N2–Rh1–S1	84.0 (3)	86.14
S1–Rh1–Cl1	100.8 (3)	98.91
S1–Rh1–Cl2	91.3 (2)	92.23
S1–Rh1–P1	86.6 (3)	88.76
Cl1–Rh1–Cl2	88.8 (4)	89.51
Cl1–Rh1–P1	86.6 (3)	88.41
Cl2–Rh1–P1	174.5 (4)	176.2

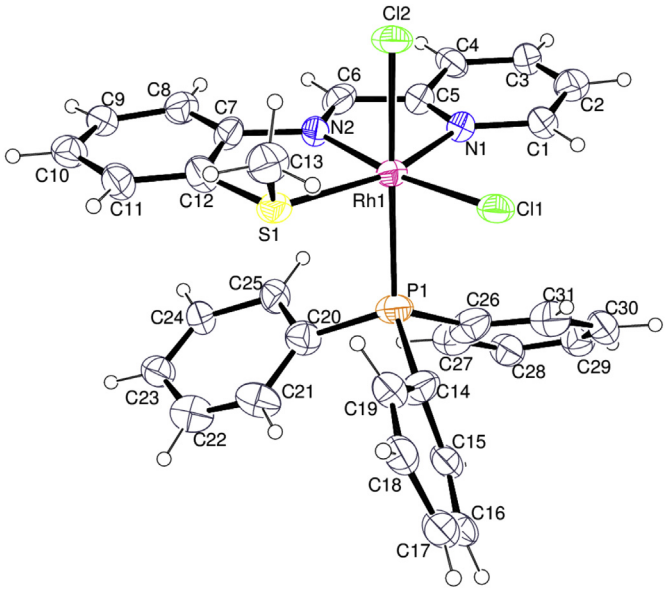

Fig. 1. ORTEP plot of $\mathbf{1}^+$ with 35% ellipsoidal probability.

nature of electronic transitions in the compound TDDFT calculation on the optimized geometry has been performed in acetonitrile using TDDFT/CPCM method. The experimental bands along with calculated vertical electronic transitions are summarized in Table 4. The peak at 418 nm corresponds to HOMO/HOMO-1 → LUMO transitions having mixed $d\pi$(Rh) → π^*(L) (metal to ligand charge transfer transition, MLCT) and $p\pi$(Cl) → π^*(L) (halogen to ligand charge transfer transition, XLCT). The calculated strong transition at 342 nm ($f = 0.2086$) corresponding to HOMO-8 → LUMO transition having mixed ILCT and XLCT character well matched with the experimental band at 330 nm. The experimental band at 270 nm again corresponds to ILCT character.

Upon excitation at 330 nm the complex **1** shows emission band at 455 nm with emission quantum yield (ϕ) = 0.031 in acetonitrile (Fig. 4). Lifetime data of the compound is taken at 298 K in acetonitrile solution when excited at 370 nm. The fluorescence decay curve was deconvoluted with respect to the lamp profile. The observed florescence decay fits with bi-exponential nature (Fig. 5). We have used mean fluorescence lifetime ($\tau_f = a_1\tau_1 + a_2\tau_2$, where a_1 and a_2 are relative amplitude of decay process) to study the excited state stability of the complex. The fluorescence lifetime of the complex is 1.78 ns in acetonitrile.

3.5. Electrochemistry

The electrochemical behavior of the complex $[Rh(PPh_3)(L)Cl_2](PF_6)$ (**1**) has been investigated by cyclic voltammetry (CV) in presence of $[NBu_4][ClO_4]$ in MeCN at scan rate 50 mV S^{-1}. The complex shows quasi-reversible oxidative response at 1.07 V along with an irreversible reduction peak at −1.05 V, positive and negative to reference electrode respectively (Ag/AgCl) in the potential range 2.0 to −2.0 V (Fig. 6). The oxidation and reduction processes have been interpreted by DFT data. The HOMO of the complexes has mixed $d\pi$(Rh) and $p\pi$(Cl) character, thus the oxidation may be proposed as oxidation of $X^- \rightarrow 1/2X_2$ which may inherently oxidize Rh(III) to Rh(IV) following a classical EC mechanism [70]. The LUMO of complex has 95% π^*(L) character and the reduction is assigned as ligand centered.

3.6. Catalytic transfer hydrogenation reactions

In transfer hydrogenation reaction hydrogen is transferred from one organic molecule to another and has great importance in organic synthesis. We chose the transfer hydrogenation of ketones in 2-propanol to our newly synthesized Rh(III) complex **1**. Table 5 shows the high efficiency (87–92%) of the reduction of ketones to their respective alcohols with 2-propanol as hydrogen donor in the

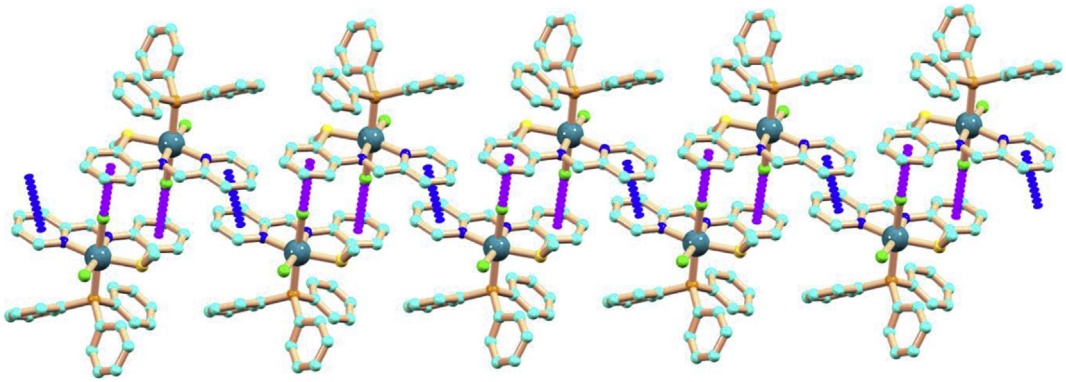

Fig. 2. 1D supramolecular chain formed by π … π (●●●) (3.390 (6) Å) and pπ(Cl) … π (●●●) (3.595(6) Å) interactions in **1**.

Table 3
Energy and composition of selected molecular orbitals of $\mathbf{1}^{+}$.

MOs	Energy (eV)	% of composition			
		Rh	L	Cl	PPh3
LUMO + 5	−3.48	01	94	0	05
LUMO + 4	−3.87	02	92	0	06
LUMO + 3	−4.32	03	94	01	02
LUMO + 2	−4.53	48	28	18	06
LUMO + 1	−4.72	41	20	14	25
LUMO	−5.97	03	95	01	01
HOMO	−9.00	16	01	62	21
HOMO-1	−9.14	24	09	57	10
HOMO-2	−9.17	20	03	46	31
HOMO-3	−9.21	09	02	37	52
HOMO-4	−9.27	02	01	10	87
HOMO-5	−9.36	21	06	54	19
HOMO-6	−9.41	04	04	09	83
HOMO-7	−9.59	08	14	20	58
HOMO-8	−9.73	02	41	10	47
HOMO-9	−9.86	01	10	03	86
HOMO-10	−9.99	02	31	02	65

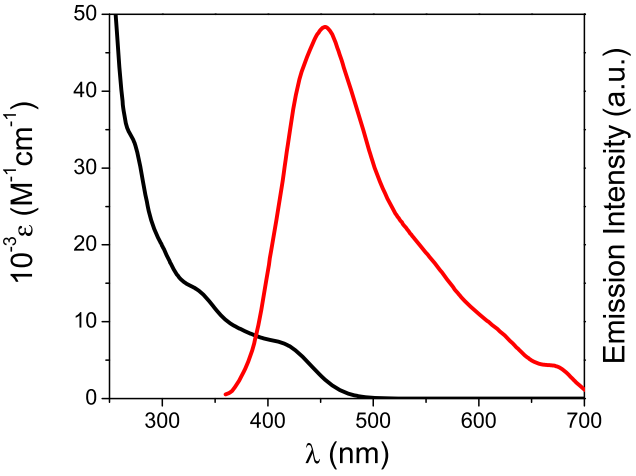

Fig. 4. Absorption (—) and emission (—) spectra ($\lambda_{emission}$ = 455 nm, $\lambda_{excitation}$ = 330 nm, quantum yield (ϕ) = 0.031) of **1** in acetonitrile.

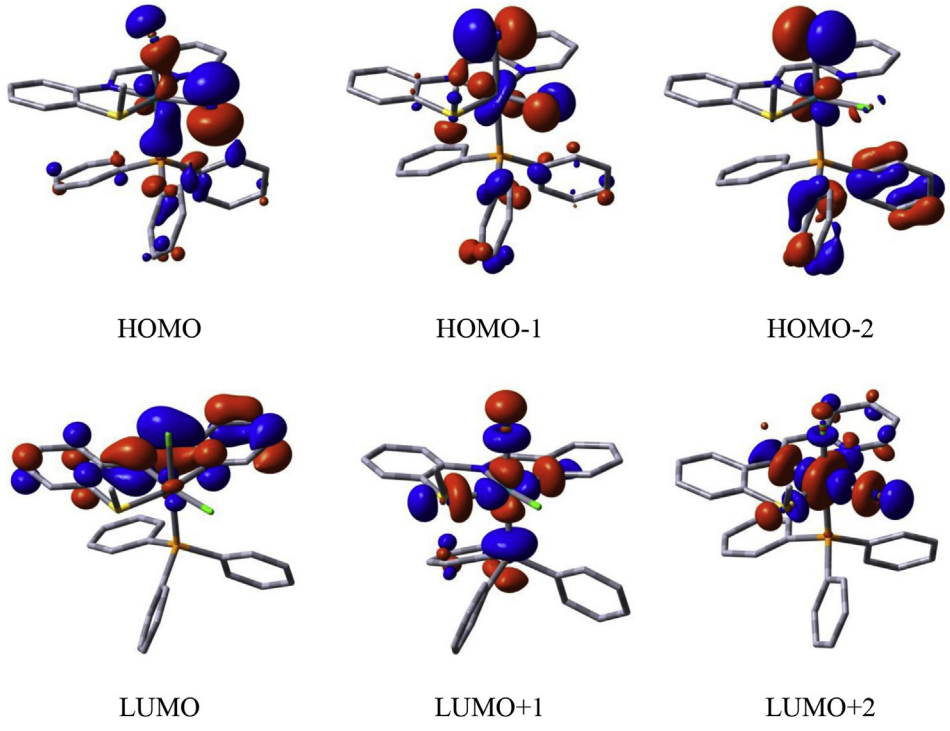

Fig. 3. Contour plots of selected molecular orbitals of $\mathbf{1}^{+}$.

Table 4
Vertical electronic excitations of **1** calculated by TDDFT/CPCM method.

$E_{excitation}$ (eV)	$\lambda_{excitation}$ (nm)	Osc. strength (f)	Key transitions	Character	$\lambda_{expt.}$ (M^{-1} cm^{-1})
2.8914	429	0.0026	(87%)HOMO → LUMO	$d\pi$(Rh)/$p\pi$(Cl) → π^*(L)	418 (7147)
2.9214	424	0.0296	(73%)HOMO-1 → LUMO	$d\pi$(Rh)/$p\pi$(Cl) → π^*(L)	
3.0583	405	0.0147	(79%)HOMO-5 → LUMO	$d\pi$(Rh)/$p\pi$(Cl) → π^*(L)	
3.6221	342	0.2086	(62%)HOMO-8 → LUMO	π(L)/$p\pi$(Cl) → π^*(L)	330 (14495)
4.1710	297	0.0817	(48%)HOMO-8 → LUMO + 1 (29%)HOMO-10 → LUMO + 1	π(L)/π(PPh_3) → $d\pi$(Rh)/π^*(L)	273 (33582)
4.2313	293	0.0602	(43%)HOMO-13 → LUMO (32%)HOMO-8 → LUMO + 1	π(L) → π^*(L)	

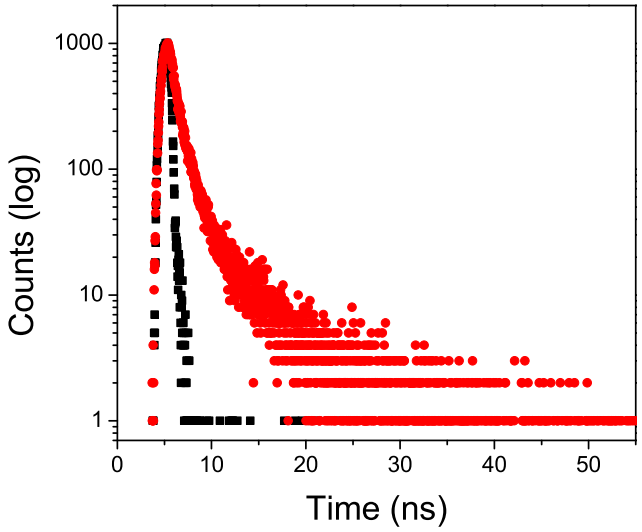

Fig. 5. Exponential decay profile of **1** in acetonitrile.

presence of KOH. The most efficient conversion has been found in the case of acetophenone (92%). In the catalytic cycle probably the Rh—Cl bond is cleaved and formation of an intermediate complex having Rh—H bond is taking place which is then effectively reduced the ketones to their corresponding alcohols [42].

3.7. Catalytic oxidation of alcohols

For the oxidation of alcohols using oxygen or hydrogen peroxide as an oxidant number of transition-metal complexes have been used as catalyst [71,72]. Oppenauer-type oxidation of alcohols in which acetone has been used as an oxidant is also a promising methods for the oxidation [73]. Herein, we have examined the oxidation of alcohols using NMO as co-oxidant in CH_2Cl_2 catalyzed by new Rh(III) complex **1**. The complex efficiently catalyzes the oxidation of 2-butanol to 2-butanone, benzyl alcohol to benzaldehyde, 1-phenylethanol to acetophenone, cyclopentanol to cyclopentanone, cyclohexanol to cyclohexanone, cycloheptanol to cycloheptanone and cycloctanol to cycloctanone with moderate to high conversions (79—85%) and the results are summarized in Table 6. Blank experiments established that each component is essential for an effective catalytic transformation and the oxidation did not take place under aerial O_2 in absence of NMO and/or Rh(III) complexes.

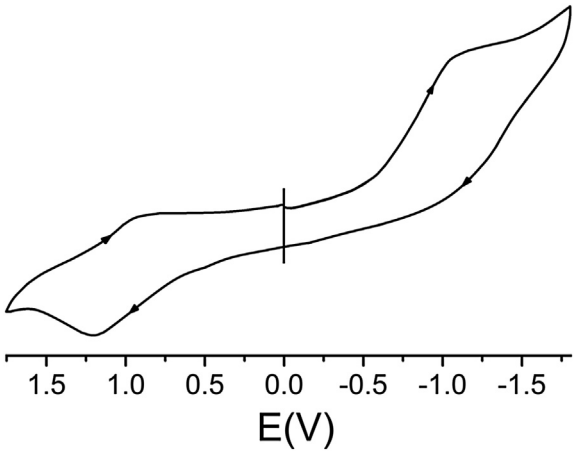

Fig. 6. Cyclic voltammogram of **1** in acetonitrile.

Table 5
Transfer hydrogenation of ketones by Rh(III) complex **1**.

Substrate	Product	Conversion (%)
Cyclopentanone	Cyclopentanol	91
Cyclohexanone	Cyclohexanol	87
Acetophenone	1-Phenylethanol	92
2-Butanone	2-Butanol	87

3.8. Powder XRD

The experimental PXRD pattern of the bulk product of **1** is in good agreement with the simulated XRD patterns from single-crystal X-ray diffraction result, indicating consistency of the bulk sample (Fig. S2). The simulated patterns of the complexes were calculated from the single crystal structural data (Cif files) using the CCDC Mercury software.

4. Conclusion

New rhodium(III)-triphenylphosphine complex, [Rh(PPh_3)(L)Cl_2](PF_6) (**1**) with thioether containing NNS donor ligand (L) (L = 2-(methylthio)-N-((pyridine-2-yl)methylene)benzenamine) has been synthesized and characterized by both experimental and theoretical studies. The electrochemical properties of the complexes have been examined and supported by DFT data. The spin allowed

Table 6
Catalytic oxidation of alcohols by Rh(III) complex **1** using NMO as co-oxidant.

Substrate	Product	Conversion (%)
2-Butanol	2-Butanone	79
Benzyl alcohol	Benzaldehyde	79
1-Phenylethanol	Acetophenone	81
Cyclopentanol	Cyclopentanone	82
Cyclohexanol	Cyclohexanone	85
Cycloheptanol	Cycloheptanone	83
Cycloctanol	Cycloctanone	82

electronic transitions computed by TDDFT method have a good agreement with the experimental spectra. The complex effectively catalyzed the transfer hydrogenation reaction of ketones with high yields (87–92%) in 2-propanol. The catalytic oxidations of alcohols in presence of NMO give moderate to high yield (79–85%).

Acknowledgment

Financial supports received from the Department of Science and Technology, New Delhi, India (No. SB/EMEQ–242/2013) is gratefully acknowledged. S. Biswas and P. Roy are thankful to UGC, New Delhi, India and D. Sarkar thanks CSIR, New Delhi, India for fellowship.

Appendix A. Supplementary data

Supplementary data related to this article can be found at http://dx.doi.org/10.1016/j.molstruc.2015.06.065.

References

[1] C. Piguet, G. Bernardinelli, G. Hopfgartner, Chem. Rev. 97 (1997) 2005–2062.
[2] U. Knof, A. von Zelewsky, Angew. Chem. Int. Ed. 38 (1999) 303–322.
[3] K. Kalyanasundaram, M. Grätzel, Coord. Chem. Rev. 177 (1998) 347–418.
[4] V. Balzani, A. Juris, M. Venturi, S. Campagna, S. Serroni, Chem. Rev. 96 (1996) 759–834.
[5] A.B. Tamayo, S. Garon, T. Sajoto, P.I. Djurovich, I.M. Tsyba, R. Bau, M.E. Thompson, Inorg. Chem. 44 (2005) 8723–8732.
[6] F. Hua, S. Kinayyigit, A.A. Rachford, E.A. Shikhova, S. Goeb, J.R. Cable, C.J. Christopher, K. Kirschbaum, A.A. Pinkerton, F.N. Castellano, Inorg. Chem. 46 (2007) 8771–8783.
[7] X. Wang, T. Kenny, D. Fortin, S.M. Aly, G. Brisard, P.D. Harvey, Organometallics 34 (2015) 1567–1581.
[8] M. Gratzel, Energy Resources through Photochemistry and Catalysis, Academic, New York, 1983.
[9] S.S. Jurisson, J.D. Lydon, Chem. Rev. 99 (1999) 2205–2218.
[10] W.A. Volkert, T.J. Hoffman, Chem. Rev. 99 (1999) 2269–2292.
[11] I.R. Farrell, A. Vlček Jr., Coord. Chem. Rev. 208 (2000) 87–101.
[12] A. Vogler, H. Kunkely, Coord. Chem. Rev. 200–202 (2000) 991–1008.
[13] F. Li, G. Cheng, Y. Zhao, J. Feng, S. Liu, M. Zhang, Y. Ma, J. Shen, Appl. Phys. Lett. 83 (2003) 4716–4718.
[14] A. Vlček Jr., M. Busby, Coord. Chem. Rev. 250 (2006) 1755–1762.
[15] W.B. Connick, A. Di Bilio, M.G. Hill, J.R. Winkler, H.B. Gray, Inorg. Chim. Acta 240 (1995) 169–173.
[16] K.K.-W. Lo, K.H.-K. Tsang, W.K. Hui, N. Zhu, Chem. Commun. (2003) 2704–2705.
[17] A.R. Dunn, W. Belliston-Bittner, J.R. Winkler, E.D. Getzoff, D.J. Stuehr, H.B. Gray, J. Am. Chem. Soc. 127 (2005) 5169–5179.
[18] S. Mardanya, S. Karmakar, D. Maity, S. Baitalik, Inorg. Chem. 54 (2015) 513–526.
[19] K. Wang, L. Huang, L. Gao, L. Jin, C. Huang, Inorg. Chem. 41 (2002) 3353–3358.
[20] Z. Si, J. Li, B. Li, F. Zhao, S. Liu, W. Li, Inorg. Chem. 46 (2007) 6155–6163.
[21] S. Karmakar, S. Mardanya, S. Das, S. Baitalik, J. Phys. Chem. C 119 (2015) 6793–6805.
[22] M. Rombach, J. Seebacher, M. Ji, G. Zhang, G. He, M.M. Ibrahim, B. Benkmil, H. Vahrenkamp, Inorg. Chem. 45 (2006) 4571–4576.
[23] L.M. Berreau, Eur. J. Inorg. Chem. (2006) 273–283.
[24] F. Thomas, Eur. J. Inorg. Chem. (2007) 2379–2404.
[25] L. Zhou, D. Powell, K.M. Nicholas, Inorg. Chem. 46 (2007) 7789–7799.
[26] R.A. Allred, S.A. Hufner, K. Rudzka, A.M. Arif, L.M. Berreau, Dalton Trans. (2007) 351–357.
[27] M.R. Malachonsk, M. Adams, N. Elia, A.L. Rheingold, R.S. Kelly, J. Chem. Soc. Dalton Trans. (1999) 2177–2182.
[28] B. Adhikary, S. Liu, C.R. Lucas, Inorg. Chem. 32 (1993) 5957–5962.
[29] P. Chakraborty, S.K. Chandra, A. Chakravorty, Inorg. Chem. 32 (1993) 5349–5353.
[30] A. Karmakar, S.B. Chaoudhury, A. Chakrovorty, Inorg. Chem. 33 (1994) 6148–6153.
[31] K. Pramanik, S. Karmakar, S.B. Choudhury, A. Chakravorty, Inorg. Chem. 36 (1997) 3562–3564.
[32] S. Mukhopadhyay, D. Ray, J. Chem. Soc. Dalton Trans. (1995) 265–268.
[33] A.K. Singh, R. Mukherjee, Dalton Trans. (2005) 2886–2891.
[34] M.S. Jana, A.K. Pramanik, S. Kundu, T.K. Mondal, Polyhedron 40 (2012) 46–52.
[35] M.S. Jana, A.K. Pramanik, S. Kundu, D. Sarkar, S. Jana, T.K. Mondal, Inorg. Chim. Acta 394 (2013) 583–590.
[36] T.K. Mondal, P. Raghavaiah, A.K. Patra, C. Sinha, Inorg. Chem. Commun. 13 (2010) 273–277.
[37] T.K. Mondal, J.-S. Wu, T.-H. Lu, Sk Jasimuddin, C. Sinha, J. Organomet. Chem. 694 (2009) 3518–3525.
[38] G. Venkatachalam, R. Ramesh, Inorg. Chem. Commun. 9 (2006) 703–707.
[39] D. Serkan, N.K. Ozpozan, N. Ozdemir, O. Dayan, J. Organomet. Chem. 770 (2014) 21–28.
[40] X.-H. Zhu, L.-H. Cai, C.-X. Wang, Y.-N. Wang, X.-Q. Guo, X.-F. Hou, J. Mol. Catal. A Chem. 393 (2014) 134–141.
[41] G. Prakash, P. Viswanathamurthi, Spectrochem. Acta. A 129 (2014) 352–358.
[42] O. Prakash, P. Singh, G. Mukherjee, A.K. Singh, Organometallics 31 (2012) 3379–3388.
[43] O. Prakash, H. Joshi, K.N. Sharma, P.L. Gupta, A.K. Singh, Organometallics 33 (2014) 3804–3818.
[44] R.S. Drago, Coord. Chem. Rev. 117 (1992) 185–213.
[45] T. Iwasawa, M. Tokunaga, Y. Obora, Y. Tsuji, J. Am. Chem. Soc. 126 (2004) 6554–6555.
[46] Y. Uozumi, R. Nakao, H. Rhee, J. Organomet. Chem. 692 (2007) 420–427.
[47] K. Mori, T. Hara, T. Mizugaki, K. Ebitani, K. Kaneda, J. Am. Chem. Soc. 126 (2004) 10657–10666.
[48] H.-K. Kwong, P.-K. Lo, K.-C. Lau, T.-C. Lau, Chem. Commun. 47 (2011) 4273–4275.
[49] H.R. Mardani, H. Golchoubian, Tetrahedron Lett. 47 (2006) 2349–2352.
[50] P. Singh, A.K. Singh, Organometallics 29 (2010) 6433–6442.
[51] B. Valuer, Molecular Fluorescence: Principles and Applications, Wiley-VCH, Weinheim, 2001.
[52] A.D. Becke, J. Chem. Phys. 98 (1993) 5648–5652.
[53] C. Lee, W. Yang, R.G. Parr, Phys. Rev. B 37 (1988) 785–789.
[54] P.J. Hay, W.R. Wadt, J. Chem. Phys. 82 (1985) 270–283.
[55] W.R. Wadt, P.J. Hay, J. Chem. Phys. 82 (1985) 284–298.
[56] P.J. Hay, W.R. Wadt, J. Chem. Phys. 82 (1985) 299–310.
[57] M.J. Frisch, G.W. Trucks, H.B. Schlegel, G.E. Scuseria, M.A. Robb, J.R. Cheeseman, G. Scalmani, V. Barone, B. Mennucci, G.A. Petersson, H. Nakatsuji, M. Caricato, X. Li, H.P. Hratchian, A.F. Izmaylov, J. Bloino, G. Zheng, J.L. Sonnenberg, M. Hada, M. Ehara, K. Toyota, R. Fukuda, J. Hasegawa, M. Ishida, T. Nakajima, Y. Honda, O. Kitao, H. Nakai, T. Vreven, J.A. Montgomery Jr., J.E. Peralta, F. Ogliaro, M. Bearpark, J.J. Heyd, E. Brothers, K.N. Kudin, V.N. Staroverov, R. Kobayashi, J. Normand, K. Raghavachari, A. Rendell, J.C. Burant, S.S. Iyengar, J. Tomasi, M. Cossi, N. Rega, J.M. Millam, M. Klene, J.E. Knox, J.B. Cross, V. Bakken, C. Adamo, J. Jaramillo, R. Gomperts, R.E. Stratmann, O. Yazyev, A.J. Austin, R. Cammi, C. Pomelli, J.W. Ochterski, R.L. Martin, K. Morokuma, V.G. Zakrzewski, G.A. Voth, P. Salvador, J.J. Dannenberg, S. Dapprich, A.D. Daniels, Ö. Farkas, J.B. Foresman, J.V. Ortiz, J. Cioslowski, D.J. Fox, Gaussian 09, Revision D.01, Gaussian, Inc., Wallingford CT, 2009.
[58] R. Bauernschmitt, R. Ahlrichs, Chem. Phys. Lett. 256 (1996) 454–464.
[59] R.E. Stratmann, G.E. Scuseria, M.J. Frisch, J. Chem. Phys. 109 (1998) 8218–8224.
[60] M.E. Casida, C. Jamorski, K.C. Casida, D.R. Salahub, J. Chem. Phys. 108 (1998) 4439–4449.
[61] V. Barone, M. Cossi, J. Phys. Chem. A 102 (1998) 1995–2001.
[62] M. Cossi, V. Barone, J. Chem. Phys. 115 (2001) 4708–4717.
[63] M. Cossi, N. Rega, G. Scalmani, V. Barone, J. Comput. Chem. 24 (2003) 669–681.
[64] N.M. O'Boyle, A.L. Tenderholt, K.M. Langner, J. Comput. Chem. 29 (2008) 839–845.
[65] G.M. Sheldrick, SHELX97, Programs for Crystal Structure Analysis (Release 97–2), University of Göttingen, Göttingen, Germany, 1997.
[66] M. Hirotsu, A. Kobayashi, T. Yoshimura, T. Konno, J. Chem. Soc. Dalton Trans. (2002) 878–884.
[67] M. Hirotsu, A. Kobayashi, T. Yoshimura, T. Konno, J. Chem. Soc. Dalton Trans. (2002) 878–884.
[68] A. Labande, J.-C. Daran, N.J. Long, A.J.P. White, R. Poli, New. J. Chem. 35 (2011) 2162–2168.
[69] D. Sardar, P. Datta, P. Mitra, C. Sinha, Polyhedron 29 (2010) 3170–3177.
[70] S. Jana, M.S. Jana, S. Biswas, C. Sinha, T.K. Mondal, J. Mol. Struct. 1065–1066 (2014) 52–60.
[71] D.R. Jensen, M.J. Schultz, J.A. Mueller, M.S. Sigman, Angew. Chem. Int. Ed. 42 (2003) 3810–3813.
[72] T. Iwasawa, M. Tokunaga, Y. Obora, Y. Tsuji, J. Am. Chem. Soc. 126 (2004) 6554–6555.
[73] F. Hanasaka, K. Fujita, R. Yamaguchi, Organometallics 25 (2004) 1490–1492.